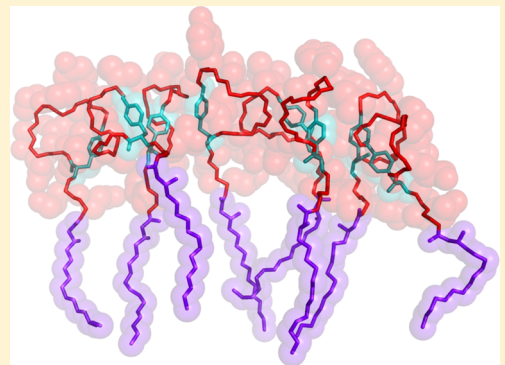


Selectivity and Mechanism of Fengycin, an Antimicrobial Lipopeptide, from Molecular Dynamics

Sreyoshi Sur,[†] Tod D. Romo,[‡] and Alan Grossfield^{*,§}[†]Department of Chemistry, University of Rochester, 404 Hutchison Hall, Box 270216, Rochester, New York 14627, United States[‡]Center for Integrated Research Computing, University of Rochester, 601 Elmwood Avenue, Box 712, Rochester, New York 14642, United States[§]Department of Biochemistry and Biophysics, University of Rochester Medical Center, Rochester, 601 Elmwood Avenue, Box 712, New York 14642, United States

Supporting Information

ABSTRACT: Fengycin is a cyclic lipopeptide used as an agricultural fungicide. It is synthesized by *Bacillus subtilis* as an immune response against fungal infection and functions by damaging the target's cell membrane. Previous molecular dynamics simulations and experiments have led to the hypothesis that the aggregation of fengycins on the membrane surface plays a key role in cell disruption. Here, we used microsecond-scale all-atom molecular dynamics simulations to understand the specificity, selectivity, and structure of fengycin oligomers. Our simulations suggest that fengycin is more likely to form stable oligomers in model fungal membranes (phosphatidylcholine) compared to the model bacterial membranes (phosphatidylethanolamine:phosphatidylglycerol). Furthermore, we characterize the differences in the structure and kinetics of the membrane-bound aggregates and discuss their functional implications.



INTRODUCTION

Lipopeptides are a class of antibiotics that can effectively act against a plethora of disease-causing organisms.¹ Many are expressed by bacteria and can have both antibacterial and antifungal activities. Fengycin, along with surfactins and iturins, is a member of a family of cyclic lipopeptides originally obtained from *Bacillus subtilis*. These bacteria grow synergistically in the roots of leguminous plants, where they protect them from phytopathogens.² Fengycin acts as a fungicide and can be used to treat various diseases in plants like clubroot disease (*Plasmiodiophora moniliforme*), maize rot (*Fusarium moniliforme*), barley head blight (*Fusarium graminearum*), and cucurbit powdery (*Podosphaera fusca*).^{3–5} Biocontrol agents like fengycin avoid the adverse effects of chemical pesticides and are ecofriendly. Through genetic modifications, certain strains of *B. subtilis* are capable of overproducing lipopeptides, which led to the development of the commercially available biofungicide Serenade (Bayer).

There are two methods by which fengycin acts against these fungi. First, it induces a systemic resistance in the plants by perturbing the cell membrane of the root cells.^{1,8} Second, fengycin directly attacks the fungi by binding to their cell membrane, causing leakage and lysis.^{9–12} In this work, we will focus on the latter phenomenon.

Beyond its established agricultural applications, fengycin (and related compounds) show promise as antifungal drugs. Fengycin has a low hemolytic activity, and the combination of D-amino acids and cyclic structure makes it less vulnerable to

degradation by peptidases compared to conventional antimicrobial peptides.³ Furthermore, membrane composition varies slowly in an evolutionary sense, slowing the advent of fungal resistance. In addition, fengycin has been found to be effective against filamentous fungi and hypothesized to be effective against localized dermatomycosis.^{13,14} After the approval of daptomycin, present in the drug Cubicin, increasing efforts to find lipopeptide-based drugs have increased.¹⁵ Thus, understanding how fengycin interacts with the bilayers will help us understand how best to use it as a basis for future drug development.

Coarse-grained molecular dynamics simulations of individual and oligomerized fengycins in various lipid bilayers suggest that they bind to all of the membranes with their acyl chains inserted into the hydrophobic core.¹⁶ These simulations also show that the membrane composition affects fengycin's tendency to aggregate in the membrane; specifically, the aggregates are stable in bilayers made with phosphatidylcholine (PC) head groups (typical of eukaryotic cells), but not in bacterium-like mixtures of phosphatidylethanolamine (PE) and phosphatidylglycerol (PG). The authors hypothesize that the aggregates, which significantly bend and distort the membrane, are the active form of the lipopeptide. These results are highly suggestive, but the limitations of a coarse-grained force field in

Received: December 1, 2017

Revised: January 25, 2018

Published: January 27, 2018

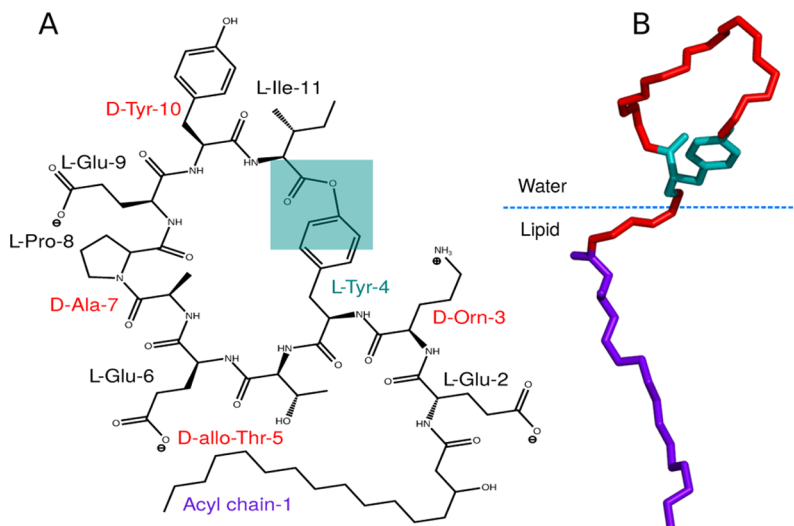


Figure 1. (A) Chemical structure of fengycin (adapted from Horn et al.);^{16,17} (B) three-dimensional orientation of one of the conformations of fengycin during our simulation. Violet sticks represent the acyl tail, red sticks show the peptide backbone, and cyan sticks stand for the C-terminus and Tyr-4 ester linkage.

representing detailed packing and electrostatic interactions require that they be confirmed by all-atom simulations, particularly given the number of charged moieties in the system.

The goal of the present work is to clarify the composition-specific effects of fengycin on model lipid bilayers chosen to mimic eukaryotic and bacterial membranes via all-atom molecular dynamics simulations. The simulations demonstrate statistically significant differences between the lipopeptides' behavior depending on the nature of the lipid head groups, with the resulting differences in their effects on bilayer structure.

METHODS

Chemical Structure of Fengycin. Fengycin is an amphipathic cyclic lipopeptide, with the chemical structure as shown in Figure 1. It consists of an anionic cyclic decapeptide with a β -hydroxy fatty acid attached at the N-terminus.¹⁶ Fengycin naturally occurs with a number of variations in the protein sequence and acyl chain length; the specific fengycin used in the present simulations was first reported by Wu et al. and characterized by Pathak et al. using mass spectroscopic techniques.^{17,18} This particular variant has several distinctive features: (i) four D-amino acid residues (tyrosine (Tyr-10), alanine (Ala-7), non-natural ornithine (Orn-3), and threonine (Thr-5)); (ii) three negatively charged glutamate (Glu-2, Glu-6, and Glu-9) residues and one positively charged residue Orn-3, resulting in a net charge of -2 ; and (iii) cyclic structure with the ring closure occurring between Tyr-4 and Ile-11 through an ester bond.

System Construction. Fengycin has some unusual moieties not found in the standard CHARMM36 force field, including the β -hydroxyl on the acyl chain and the ester bond connecting the C-terminus to Tyr-4. Parameters for these atoms were developed using the Forcefield toolkit plugin to VMD.^{19,20} A stream file (feng_stream.txt) containing all of the new parameters is attached as the [Supporting Information](#). The lipopeptide structures were built using a modeling tool, Molefactory, which is found as an extension of VMD.²⁰

We constructed a membrane-bound fengycin system by placing molecules randomly on two planes parallel to the z -axis,

with the acyl chains pointing toward the membrane center, producing systems with 10 lipopeptides in each leaflet. The choice to run symmetric systems was an attempt to model the long-time equilibrium behavior accessible to experiments such as the fluorescence work from Heerklotz and co-workers.¹⁰ However, this choice did mean that membrane deformations due to asymmetric binding were not accessible; some antimicrobial peptides seem to exploit that asymmetry to induce pores, with the result that at long times, their activity goes away due to peptide migration to the inner leaflet.²¹

The Optimal Membrane Generator package from LOOS was used to place lipids around fengycin and solvate the system.^{22,23} The system was electronically neutralized with excess sodium ions, with the additional NaCl added to bring the free salt concentration to approximately 100 mM. We modeled the water using TIP3P, as was appropriate with the CHARMM force field. The system was thoroughly minimized and equilibrated through a series of alternating minimizations and short dynamics runs.

Table 1 summarizes the different systems run. To model the Gram-negative bacteria, we used a 2:1 mixture of palmitoyl-

Table 1. Summary of Simulations

system	phospholipids	fengycins per leaflet	length (ns)	# of replicates
bacteria	PE:PG	10	\sim 5000	4
fungus	PC	10	\sim 4500	4
neat	PE:PG	0	\sim 150	3
neat	PC	0	\sim 150	3

oleoyl-phosphatidylethanolamine (PE) and palmitoyl-oleoyl-phosphatidylglycerol (PG). A pure palmitoyl-oleoyl-phosphatidylcholine (PC) bilayer was used to emulate a eukaryotic membrane. The lipopeptide–lipid systems had 10 fengycins bound to each leaflet of the lipid bilayer. As a control, we ran simulations of neat bilayers with the same compositions. For each lipopeptide system, we ran four independently constructed replicates, whereas for the pure lipid systems, we ran three replicates of each. All of the systems had 90 lipids per leaflet.

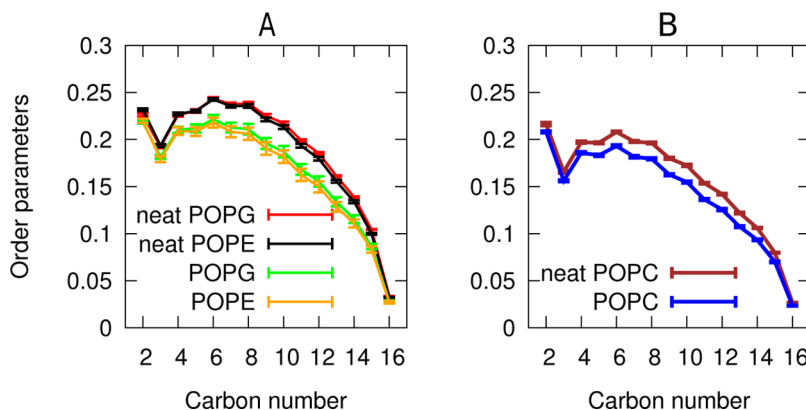


Figure 2. Order parameters for the palmitoyl chain of (A) PE:PG and (B) PC. Neat indicates order parameters for membrane systems without any fengycin in them. The error bars indicate the standard error for each replicate. Carbon number for the palmitoyl chain is along the *x*-axis, whereas the average order parameter is along the *y*-axis.

Simulation Protocol. All of the simulations were run with a NAMD version 2.9.²⁴ We used the CHARMM36 force field for both the peptide and lipid, including the CMAP correction for the peptide backbone; the D-amino acids were represented by defining a new atom type for the D- α carbon and transposing the matrices for the CMAP values (see the parameters for D-Orn in the *Supporting Information*).^{25–28}

We used Langevin dynamics for all of the heavy atoms with the temperature set at 310.5 K, and the Langevin piston barostat with semi-isotropic boundary conditions.^{29–31} We used a smooth particle-mesh Ewald summation with a $96 \times 96 \times 96$ grid to calculate the long-range electrostatics.³² van der Waals interactions were smoothly cutoff from 8 to 12 Å, with the pairlist maintained at 14 Å. We used a 2 fs timestep, with the bonds constrained to their equilibrium lengths using the RATTLE algorithm.³³

Simulation Analysis. All of the analyses were done at 1 ns resolution unless otherwise specified. For equilibration purposes, we excluded the first 500 ns of the lipopeptide simulations and 100 ns of the pure membrane simulation. All of the analyses were performed with tools developed using LOOS, a software package for the analysis of molecular dynamics simulations, available for download from <https://github.com/GrossfieldLab/loos>.^{22,34} Unless otherwise noted, all of the error bars were standard errors in the mean, computed by treating each trajectory as an individual measurement.

Radial Distribution Functions. We determined the three-dimensional radial distribution functions for various pairs of atoms using the atomic_rdf tool from LOOS.^{22,34} We also calculated the radial distribution function in the membrane plane for fengycin and the different lipid species using the xy_rdf tool, also a part of LOOS; this tool operated on the molecules' centers of mass, rather than individual atoms. The time evolution of these radial distribution functions (RDFs) was also calculated by dividing the trajectory into 10 ns windows, and the resulting figure can be found in the *Supporting Information*.

Quantifying Aggregation. We considered 2 lipopeptide molecules to be in contact if there were at least 10 pairs of heavy atoms within 3 Å of each other. Using this criterion, we calculated the number of lipopeptides in each aggregate and determined the probability distribution of aggregate size. We normalized the distribution by calculating the fraction of lipopeptides that are present in different aggregate size.

Residue–Residue Contact Map. We quantify the lipopeptide–lipopeptide interactions using the residue contact maps. The definition of a contact is similar to that described above: 2 residues are in contact if they share at least 10 pairs of heavy atoms within 3 Å. Fractional contacts are defined as the probability of a specific residue–residue pair being in contact, given that the two molecules are in contact.

Lifetime of the Aggregates. To characterize the kinetic stability of differently sized aggregates, we created a time series for each trajectory, assigning each frame a value of 1 when a particular aggregate was present, and 0 if it was not. We then calculated the autocorrelation function for each such time series and averaged the resulting correlation functions as a function of aggregate size.

Order Parameters. To quantify the effects of fengycin on lipid chain structure, we computed the order parameters analogous to those measurable via solid-state deuterium quadrupolar splitting experiments. The order parameters are calculated using the second Legendre polynomial applied to the angle θ between a given acyl carbon–hydrogen bond and the membrane normal

$$S_{CD} = \left| \left\langle \frac{1}{2}(3 \cos^2 \theta - 1) \right\rangle \right| \quad (1)$$

This calculation was performed using the order_params tool from LOOS.^{22,34}

Molecular Order Parameters. To characterize the length scale on which fengycin alters the lipid chain structure, we calculated the molecular order parameters for lipid chains as a function of distance to the nearest fengycin, using the LOOS tool dibmops.^{22,34} Analogous to the deuterium order parameter shown in eq 1, the molecular order parameter is the second Legendre polynomial of the angle between the membrane normal and the average of the second and third principal axes of the chain.

RESULTS AND DISCUSSION

Fengycin Causes Disorder in Membrane. One of the most common effects of antimicrobial peptides is to reduce the order of the surrounding lipids.³⁵ To quantify this, we compute the order parameter profiles for the lipid palmitoyl chains, as described in section **Order Parameters** under **Methods**, with the results shown in Figure 2. As expected, fengycin reduces the order parameters for all of the carbons between C-3 and C-15

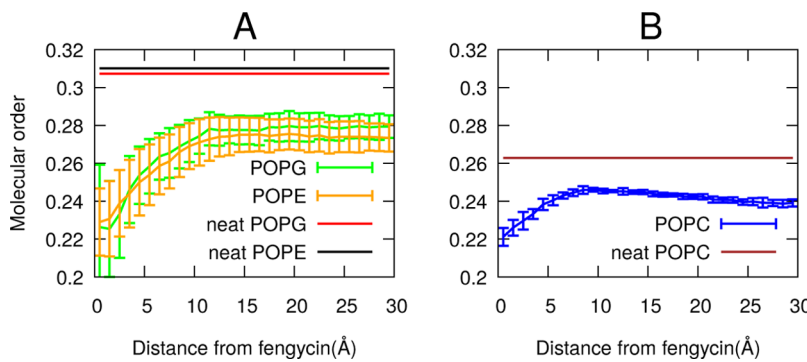


Figure 3. Molecular order parameters of palmitoyl chain as a function of distance from fengycin molecule: (A) for PE:PG and (B) for PC. The error bars are the standard error for each replicate. Neat membranes (no fengycins) are represented as straight lines.

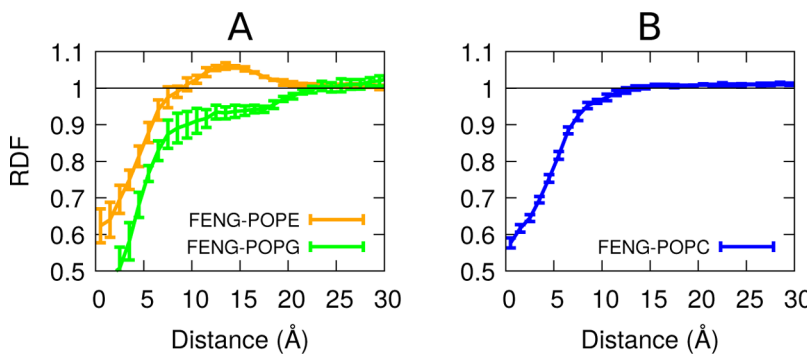


Figure 4. Radial distribution function in the membrane plane between fengycin peptide ring and the lipid head group: (A) for PE:PG and (B) for PC. Distance between the two sets of entities is along the x -axis, whereas the RDF is along the y -axis. The straight line at 1 represents the RDF value for a random distribution such as the ideal gas. The error bars are the standard error, treating each trajectory as a single measurement.

relative to their equivalents in neat membranes. This indicates an overall disordering effect but does not indicate the length-scale on which fengycin operates. To determine this, we compute the chain order parameter as a function of distance, as discussed in section **Molecular Order Parameters** under **Methods**. Figure 3 also shows that the molecular order parameter for membrane bilayers containing fengycins is lower than that for the equivalent neat membranes, consistent with Figure 2. However, the effect is most pronounced for lipids within 10 Å of the nearest fengycin, plateauing at longer range. In addition, the order parameter remains lower than the neat membrane even at a very long range; presumably, more distant lipids are altered by their disordered neighbors and not by fengycin directly.

Preferential Interaction with PE. In addition to altering the lipid chain structure, antimicrobial peptides can also alter the lateral ordering of lipid head groups.^{36,37} This is most easily quantified using a lateral radial distribution function, as shown in Figure 4. Using the method described in **Radial Distribution Functions**, we calculate the radial distribution function between the centers of mass of fengycin and different lipid types (PE, PG, PC). Figure 4A shows that PE is significantly enriched in the first solvation shell surrounding fengycin, whereas PG is equivalently depleted. By contrast, PC shows no evidence of structuring around fengycin, other than steric depletion at short range.

The apparent attraction between fengycin and PE is likely due to two factors. First, the PE amine group is a hydrogen bond donor, unlike the choline group in PC, so it can make favorable interactions with the peptide's anionic side chains. Second, electrostatic repulsion between the peptide and PG,

both of which are negatively charged, could create an apparent attraction to the zwitterionic PE head group.

Head Groups Attract Charged Fengycin Residues. To test whether there are specific interactions that attract fengycin to PE head groups, we compute a series of three-dimensional radial distribution functions as shown in Figure 5. Please note that these values are inflated by the molecules' restriction to the membrane surface. We calculate the distribution of following specific atoms: (i) nitrogens of PE amines around oxygens in

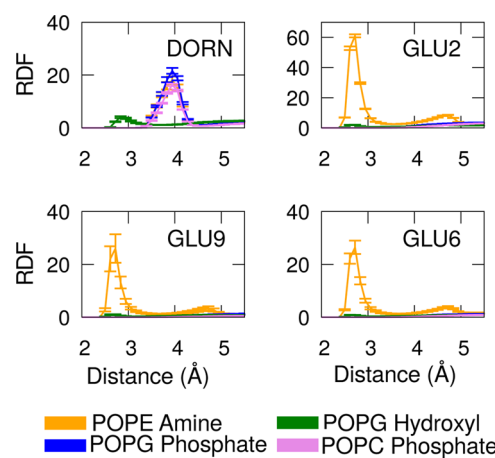


Figure 5. Three-dimensional radial distribution function between charged atoms of D-ornithine (DORN) and glutamates (GLU) in fengycin and head groups of PE, PG, and PC. RDF is along the y -axis and distance between the atoms is along the x -axis. Note the upper right panel is plotted on a different y -scale.

the carboxylate part of glutamates, (ii) oxygens of the hydroxyl group in PG glycerols around nitrogen of amine in Orn-3, and (iii) phosphates of PG and PC around nitrogen of amines in Orn-3. These atoms are selected because they indicate most likely electrostatic attractions among themselves. Figure 5 indicates that the phosphates and hydroxyls in the lipid head groups attract the positively charged ornithine side chains, whereas the three negatively charged glutamates preferentially interact with the positively charged amine of PE or with water. We do not see a net attraction between fengycin and PG because the peptide has three glutamates but only one ornithine.

Qualitatively, all of the glutamates show similar preference patterns, but quantitatively they are quite different. Glu-2 has a much higher contact peak with the PE amine, indicating it spends more time in contact than the other two glutamates. This difference is likely due to the covalent structure of fengycin; Glu-2 is immediately adjacent to the lipopeptide fatty acid, forcing the side chain to remain at the membrane–water interface. By contrast, the other two glutamates are part of the ring and can either be hydrated or interact with lipid. The lateral ordering we observe for the PE:PG section (Preferential Interaction with PE) can be rationalized by the glutamates' preferential packing with the PE amines.

Although the PC phosphates can interact favorably with ornithine (see the upper left panel of Figure 5), overall the electrostatic forces are insufficient to create a net attraction between the peptide and PC head groups (see Figure 4).

Fengycin Aggregation Depends on Membrane Composition. Our working hypothesis in performing these simulations is that the ability of fengycin to damage target membranes is related to its aggregation.¹⁶ This in turn suggests that the aggregation should vary with the bilayer's lipid composition, so that fungal (eukaryotic) membranes are damaged, whereas the native bacterial membranes are not. To test this hypothesis, we first compute the fengycin–fengycin lateral radial distribution function, shown in Figure 6.

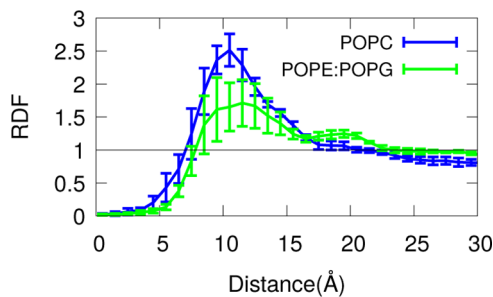


Figure 6. Lateral radial distribution function between fengycins. Lipopeptide separation is the *x*-axis, whereas the *y*-axis is the probability density. The straight line at 1 represents the RDF value for a random distribution.

The fengycin–fengycin RDF in PC shows a single large peak at roughly 10 Å, indicating a significant peptide–peptide attraction and the presence of some aggregates. Visual inspection of the trajectories confirms that the aggregates begin to appear after the first 500 ns to 1 μ s. By contrast, the first peak is significantly smaller in the PE:PG membrane, but there is a small secondary peak around 20 Å. This indicates that although there is less aggregation overall in the “bacterial

membrane”, there is a small tendency to form more elongated structures.

Characterizing Aggregate Structure. Experimental work has shown that small variations in the sequence of fengycin-like molecules can have significant effects on their activity that cannot be easily explained by changes in membrane affinity.³⁸ However, if aggregation occurred via specific structures, the mutations could plausibly disrupt the packing and reduce its favorability. Accordingly, we examine the fengycin aggregates and their tendency to form specific residue–residue contacts. Figure 7A,B shows the residue–residue contact probabilities in PC and PE:PG bilayers, respectively. Each box in the heat map represents the likelihood of specific side chain–side chain contacts within lipopeptide oligomers.

The results indicate that there is significant diversity in the ensemble of oligomeric structures; the most likely pairing (between Ile residues on each peptide) is only present in roughly 10% of the dimers. That said, there are some interesting features. The ring-closing residues (Ile and Tyr) form the strongest contacts in both membrane environments. Because these hydrophobic residues are far from the fatty acid moiety, they are less likely to be buried in the membrane; the exposed hydrophobic surface is a natural conduit for peptide–peptide interactions. This would also explain the prevalence of the D-Tyr–D-Tyr contacts and the Ile–D-Tyr contacts as well. The Tyr–Tyr contacts are also found to be higher in our all-atom simulations and in the previous coarse-grained simulation results.²⁵ Figure 7C shows an example of three fengycins in close proximity and Figure 7D zooms in to focus on the three hydrophobic residues (Tyr-4, Tyr-10, and Ile-11) that are most likely to be in contact. This indicates that tyrosines and isoleucines from adjacent fengycins can clump together. Also, this is what is observed as high contacts along the diagonal in Figure 7A,B. The other likely pairings include Glu-2 and Orn. Here, the phenomenon is largely the reverse—these charged moieties are very hydrophilic, but they are constrained to remain at the membrane–water interface because they are adjacent to the fatty acid. Formation of a charge pair could stabilize the partial dehydration required by their proximity to the membrane.

Aggregate Size is Lipid Dependent. If the tendency to aggregate is to explain the selective targeting of specific membranes, we should see a difference in the distribution of aggregate sizes between “bacteria-like” PE:PG membranes and “eukaryotic” PC membranes. Using the Quantifying Aggregation method described in Methods, we calculate the probability distribution based on the aggregate size using fengycins as the selection shown in Figure 8. Surprisingly, it looks like there is a stronger tendency to form larger aggregates (specifically, 7–8-mers) in the PE:PG membranes than in PC, in apparent contradiction with Figure 6, which indicates an overall higher probability of fengycin–fengycin pairs in PC.

This contradiction is resolved by looking at the lifetimes for different aggregate sizes, plotted in Figure 9 (see section Lifetime of the Aggregates in Methods for a discussion of how the lifetimes are computed). Figure 9 shows the autocorrelation curve for fengycin trimers (3-mers), pentamers (5-mers), and octamers (8-mers) in two different membrane systems, PE:PG and PC. In PC, trimers have the shortest lifetimes, whereas pentamers have longer lifetimes than octamers. By contrast, all of the three aggregate sizes have comparable (and very short) lifetimes in PE:PG. This indicates that small aggregates like trimers are only transient in both membranes, typically falling

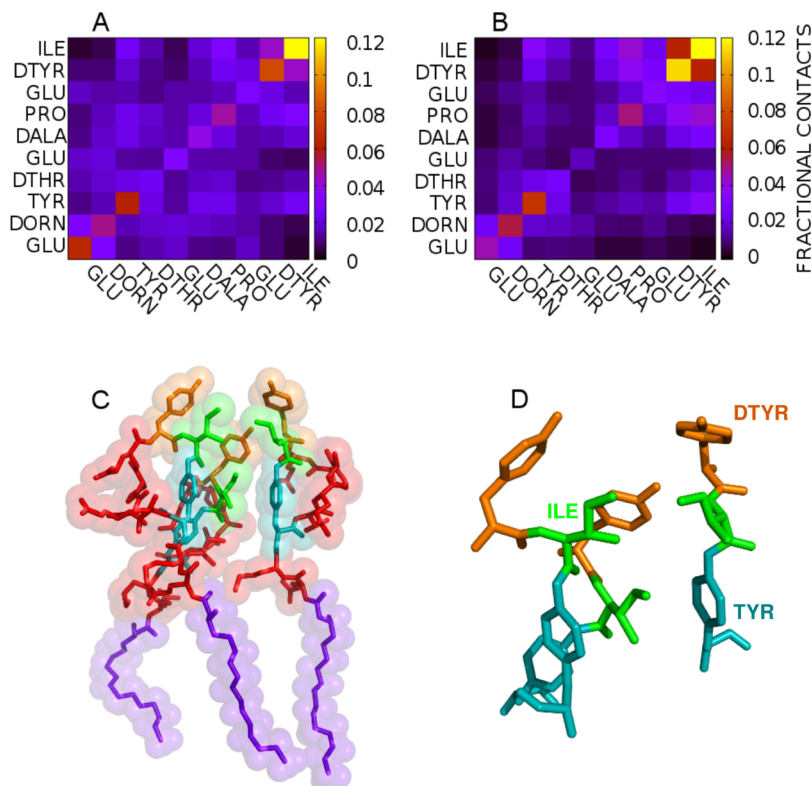


Figure 7. Fractional contacts between fengycin residues which are in contact in (A) PE:PG and (B) PC membranes. (C) Three fengycins that are in contact. (D) The residues in fengycins that have higher fractional contact value in both (A) and (B). Yellow, green, and cyan sticks represent the connectivity in heavy atoms of D-Tyr, Ile, and ring Tyr, respectively. Violet sticks show the acyl tail in fengycin and red represent the peptide bonds.

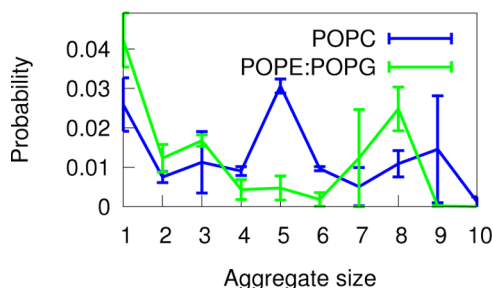


Figure 8. Probability of a specific size fengycin aggregate existing in either of the two membrane systems.

apart within 15 ns or so. In PE:PG, the lifetimes get even shorter, with all three aggregates surviving perhaps 10 ns or so. By contrast, pentamers are longer-lived in PC membranes, at

roughly 100 ns. Figure 9A shows that octamers are transient structures in the PE:PG membranes, but they are metastable in PC, as indicated by Figure 9B. The visual inspection of trajectories clarifies the difference: when larger aggregates are present in PE:PG, they are nearly always a result of “collisions” between smaller aggregates without much in the way of stabilizing interactions; as a result, they diffuse apart promptly. By contrast, when larger aggregates form in PC, they are typically stabilized by a combination of polar interactions near the membrane and hydrophobic ones far from it, as discussed above. The relative lack of significantly favorable side chain interactions with the PC head groups (compared to PE:PG) also likely contributes to the increased kinetic stability.

Going forward, we see several important questions to answer. First, the present simulations place fengycins on both membrane leaflets, essentially representing the equilibrium

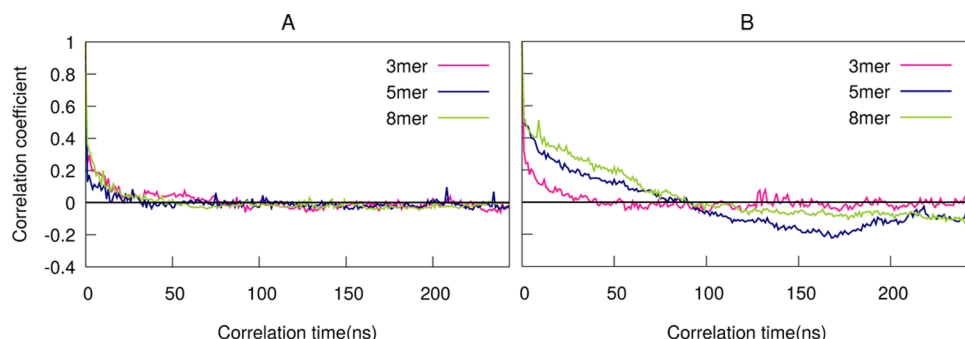


Figure 9. Lifetimes of 3-mer, 5-mer, and 8-mer in the two membrane systems: (A) PE:PG and (B) PC. Time delay is along the *x*-axis, whereas autocorrelation coefficient is along the *y*-axis.

conditions accessible in biophysical experiments. However, biologically, the fengycins would “attack” from outside the cell, initially binding exclusively to one leaflet. It is possible that the aggregation differences would be made more significant by this asymmetry, as suggested by our previous coarse-grained work.¹⁶

Second, it is extremely difficult to quantify the thermodynamics of aggregate formation on the time scales accessible to all-atom membrane simulations because equilibrium simulations would have to run long enough for aggregates to form and break up multiple times. Quantitatively understanding this thermodynamics—necessary to test the hypothesis that aggregation controls function—will instead require some form of enhanced sampling to obtain quantitative accuracy.

Finally, we know that fengycins damage the fungal membranes, but do far less damage to the mammalian membranes, even though both are eukaryotic. Given the interest in using fengycin-like molecules as potential antifungal medicines, it would be valuable to understand why they target one organism but not the other.³⁹ One likely hypothesis would be to attribute the differences to the sterol present in the fungal vs mammalian membranes (ergosterol and cholesterol respectively). Some experiments indicate that cholesterol’s tendency to increase membrane order may protect mammalian membranes, but the mechanisms are unclear and could likely be revealed by future simulations.³⁸ Similarly, the presence of different anionic lipids in fungal membranes (e.g., phosphatidylinositol) may also play a role, particularly if their behavior is different from the anionic lipids found in bacteria such as PG.

CONCLUSIONS

Fengycins operate as biological fungicides primarily by targeting and damaging the fungus’ outer membranes but leaving their plant hosts and the bacteria that produce them unharmed. We used the all-atom molecular dynamics simulations of fengycin molecules bound to two membrane compositions (PE:PG and PC) chosen as simple mimics of bacterial and eukaryotic membranes to explain this functional selectivity. In particular, we showed that although fengycin binding disorders the lipid hydrophobic region independent of the head group type, its aggregation propensities vary with lipid composition. Although aggregates form in both membrane types, larger aggregates are only stable in the eukaryotic-like membranes representative of their target fungi.

In addition, fengycin perturbed the membrane irrespective of the lipid composition, but the extent of membrane leakage was traced back to the formation of aggregates. Hence, the aggregation process itself depended on the tug of war between two favoring interactions. One is the hydrophobic interactions between Tyr-10, Tyr-4, and Ile-11 of adjacent fengycins, which led to stable aggregates and the other was the favorable electrostatic interactions between fengycin’s charged residues (glutamates and ornithine) and the lipid head groups. These two attractive and repulsive forces determined whether fengycin would form aggregates on membrane surfaces or not, and thus regulate the membrane selectivity of fengycin.

ASSOCIATED CONTENT

Supporting Information

The Supporting Information is available free of charge on the ACS Publications website at DOI: [10.1021/acs.jpcb.7b11889](https://doi.org/10.1021/acs.jpcb.7b11889).

CHARMM36 all-hydrogen Toppar file for fengycin ([TXT](#))

Time evolution of lateral radial distribution function between fengycins (Figure S1); lifetime of (A) 3-mer (B) 5-mer and (C) 8-mer in the two membrane systems (Figure S2) ([PDF](#))

AUTHOR INFORMATION

Corresponding Author

*E-mail: alan_grossfield@urmc.rochester.edu.

ORCID

Sreyoshi Sur: [0000-0001-7780-2640](#)

Notes

The authors declare no competing financial interest.

ACKNOWLEDGMENTS

Funding support from National Institute of General Medical Sciences (GM095496).

REFERENCES

- Ongena, M.; Jacques, P. *Bacillus* lipopeptides: versatile weapons for plant diseases biocontrol. *Trends Microbiol.* **2008**, *16*, 115–124.
- Ongena, M.; Jacques, P.; Touré, Y.; Destain, J.; Jabrane, A.; Thonart, P. Involvement of fengycin-type lipopeptides in the multifaceted biocontrol potential of *Bacillus subtilis*. *Appl. Microbiol. Biotechnol.* **2005**, *69*, 29–38.
- Vanittanakom, N.; Loeffler, W.; Koch, U.; Jung, G. Fengycin-a novel antifungal lipopeptide antibiotic produced by *Bacillus subtilis* F-29-3. *J. Antibiot.* **1986**, *39*, 888–901.
- Li, X.-Y.; Mao, Z.-C.; Wang, Y.-H.; Wu, Y.-X.; He, Y.-Q.; Long, C.-L. Diversity and active mechanism of fengycin-type cyclopeptides from *Bacillus subtilis* XF-1 against *Plasmodiophora brassicae*. *J. Microbiol. Biotechnol.* **2013**, *23*, 313–321.
- Hu, L. B.; Shi, Z. Q.; Zhang, T.; Yang, Z. M. Fengycin antibiotics isolated from B-FS01 culture inhibit the growth of *Fusarium moniliforme* Sheldon ATCC 38932. *FEMS Microbiol. Lett.* **2007**, *272*, 91–98.
- Chan, Y.-K.; Savard, M. E.; Reid, L. M.; Cyr, T.; McCormick, W. A.; Seguin, C. Identification of lipopeptide antibiotics of a *Bacillus subtilis* isolate and their control of *Fusarium graminearum* diseases in maize and wheat. *BioControl* **2009**, *54*, 567–574.
- Romero, D.; de Vicente, A.; Olmos, J. L.; Dávila, J. C.; Pérez-García, A. Effect of lipopeptides of antagonistic strains of *Bacillus subtilis* on the morphology and ultrastructure of the cucurbit fungal pathogen *Podosphaera fusca*. *J. Appl. Microbiol.* **2007**, *103*, 969–976.
- Ongena, M.; Jourdan, E.; Adam, A.; Paquot, M.; Brans, A.; Joris, B.; Arpigny, J.-L.; Thonart, P. Surfactin and fengycin lipopeptides of *Bacillus subtilis* as elicitors of induced systemic resistance in plants. *Environ. Microbiol.* **2007**, *9*, 1084–1090.
- Heerklotz, H.; Seelig, J. Leakage and lysis of lipid membranes induced by the lipopeptide surfactin. *Eur. Biophys. J.* **2007**, *36*, 305–314.
- Patel, H.; Tscheika, C.; Edwards, K.; Karlsson, G.; Heerklotz, H. All-or-none membrane permeabilization by fengycin-type lipopeptides from *Bacillus subtilis* {QST713}. *Biochim. Biophys. Acta, Biomembr.* **2011**, *1808*, 2000–2008.
- Deleu, M.; Paquot, M.; Nylander, T. Effect of fengycin, a lipopeptide produced by *Bacillus subtilis*, on model biomembranes. *Biophys. J.* **2008**, *94*, 2667–2679.
- Deleu, M.; Paquot, M.; Nylander, T. Fengycin interaction with lipid monolayers at the air-aqueous interface-implications for the effect of fengycin on biological membranes. *J. Colloid Interface Sci.* **2005**, *283*, 358–365.
- Eeman, M.; Deleu, M.; Paquot, M.; Thonart, P.; Dufrêne, Y. Nanoscale properties of mixed fengycin/ceramide monolayers explored using atomic force microscopy. *Langmuir* **2005**, *21*, 2505–2511.

- (14) Eeman, M.; Olofsson, G.; Sparr, E.; Nasir, M. N.; Nylander, T.; Deleu, M. Interaction of fengycin with stratum corneum mimicking model membranes: a calorimetry study. *Colloids Surf, B* **2014**, *121*, 27–35.
- (15) Raja, A.; LaBonte, J.; Lebbos, J.; Kirkpatrick, P. Daptomycin. *Nat. Rev. Drug Discovery* **2003**, *2*, 943–944.
- (16) Horn, J. N.; Romo, T. D.; Grossfield, A. Simulating the mechanism of antimicrobial lipopeptides with all-atom molecular dynamics. *Biochemistry* **2013**, *S2*, S604–S610.
- (17) Wu, C.-Y.; Chen, C.-L.; Lee, Y.-H.; Cheng, Y.-C.; Wu, Y.-C.; Shu, H.-Y.; Götz, F.; Liu, S.-T. Nonribosomal synthesis of fengycin on an enzyme complex formed by fengycin synthetases. *J. Biol. Chem.* **2007**, *282*, S608–S616.
- (18) Pathak, K. V.; Keharia, H.; Gupta, K.; Thakur, S. S.; Balaram, P. Lipopeptides from the banyan endophyte, *Bacillus subtilis* K1: mass spectrometric characterization of a library of fengycins. *J. Am. Soc. Mass Spectrom.* **2012**, *23*, 1716–1728.
- (19) Mayne, C. G.; Saam, J.; Schulten, K.; Tajkhorshid, E.; Gumbart, J. C. Rapid parameterization of small molecules using the Force Field Toolkit. *J. Comput. Chem.* **2013**, *34*, 2757–2770.
- (20) Humphrey, W.; Dalke, A.; Schulten, K. VMD: visual molecular dynamics. *J. Mol. Graphics* **1996**, *14*, 33–38.
- (21) Krauson, A. J.; He, J.; Wimley, W. C. Determining the mechanism of membrane permeabilizing peptides: identification of potent, equilibrium pore-formers. *Biochim. Biophys. Acta, Biomembr.* **2012**, *1818*, 1625–1632.
- (22) Romo, T. D.; Grossfield, A. LOOS: an extensible platform for the structural analysis of simulations. *Conf. Proc. IEEE Eng. Med. Biol. Soc.* **2009**, *2009*, 2332–2335.
- (23) Lin, D.; Grossfield, A. Thermodynamics of micelle formation and micelle-membrane fusion modulate the activity of antimicrobial lipopeptides. *Biophys. J.* **2015**, *109*, 750–759.
- (24) Phillips, J. C.; Braun, R.; Wang, W.; Gumbart, J.; Tajkhorshid, E.; Villa, E.; Chipot, C.; Skeel, R. D.; Kalé, L.; Schulten, K. Scalable molecular dynamics with NAMD. *J. Comput. Chem.* **2005**, *26*, 1781–1802.
- (25) Horn, J. N.; Cravens, A.; Grossfield, A. Interactions between fengycin and model bilayers quantified by coarse-grained molecular dynamics. *Biophys. J.* **2013**, *105*, 1612–1623.
- (26) Huang, J.; MacKerell, A. D., Jr. CHARMM36 all-atom additive protein force field: validation based on comparison to NMR data. *J. Comput. Chem.* **2013**, *34*, 2135–2145.
- (27) Best, R. B.; Zhu, X.; Shim, J.; Lopes, P. E.; Mittal, J.; Feig, M.; MacKerell, A. D., Jr. Optimization of the additive CHARMM all-atom protein force field targeting improved sampling of the backbone ϕ , ψ and side-chain χ_1 and χ_2 dihedral angles. *J. Chem. Theory Comput.* **2012**, *8*, 3257–3273.
- (28) Klauda, J. B.; Venable, R. M.; Freites, J. A.; O'Connor, J. W.; Tobias, D. J.; Mondragon-Ramirez, C.; Vorobyov, I.; MacKerell, A. D., Jr.; Pastor, R. W. Update of the CHARMM all-atom additive force field for lipids: validation on six lipid types. *J. Phys. Chem. B* **2010**, *114*, 7830–7843.
- (29) Schneider, T.; Stoll, E. Molecular-dynamics study of a three-dimensional one-component model for distortive phase transitions. *Phys. Rev. B* **1978**, *17*, 1302.
- (30) Feller, S. E.; Zhang, Y.; Pastor, R. W.; Brooks, B. R. Constant pressure molecular dynamics simulation: the Langevin piston method. *J. Chem. Phys.* **1995**, *103*, 4613–4621.
- (31) Martyna, G. J.; Tobias, D. J.; Klein, M. L. Constant pressure molecular dynamics algorithms. *J. Chem. Phys.* **1994**, *101*, 4177–4189.
- (32) Ewald, P. P. The calculation of optical and electrostatic grid potential. *Ann. Phys.* **1921**, *369*, 253–287.
- (33) Andersen, H. C. RATTLE: A “velocity” version of the SHAKE algorithm for molecular dynamics calculations. *J. Comput. Phys.* **1983**, *52*, 24–34.
- (34) Romo, T. D.; Leioatts, N.; Grossfield, A. Lightweight object oriented structure analysis: tools for building tools to analyze molecular dynamics simulations. *J. Comput. Chem.* **2014**, *35*, 2305–2318.
- (35) Heerklotz, H.; Wieprecht, T.; Seelig, J. Membrane perturbation by the lipopeptide surfactin and detergents as studied by deuterium NMR. *J. Phys. Chem. B* **2004**, *108*, 4909–4915.
- (36) Wadhani, P.; Epand, R.; Heidenreich, N.; Bürck, J.; Ulrich, A.; Epand, R. Membrane-active peptides and the clustering of anionic lipids. *Biophys. J.* **2012**, *103*, 265–274.
- (37) Epand, R. M.; Epand, R. F. Lipid domains in bacterial membranes and the action of antimicrobial agents. *Biochim. Biophys. Acta, Biomembr.* **2009**, *1788*, 289–294.
- (38) Fiedler, S.; Heerklotz, H. Vesicle leakage reflects the target selectivity of antimicrobial lipopeptides from *Bacillus subtilis*. *Biophys. J.* **2015**, *109*, 2079–2089.
- (39) Pirri, G.; Giuliani, A.; Nicoletto, S. F.; Pizzuto, L.; Rinaldi, A. C. Lipopeptides as anti-infectives: a practical perspective. *Cent. Eur. J. Biol.* **2009**, *4*, 258–273.